



Article

Quantifying the Effects of Hurricanes Irma and Maria on Coastal Water Quality in Puerto Rico using Moderate Resolution Satellite Sensors

William J. Hernández ^{1,*} , Suhey Ortiz-Rosa ², Roy A. Armstrong ², Erick F. Geiger ^{3,4}, C. Mark Eakin ³  and Robert A. Warner ⁵

¹ NOAA-EPP/Center for Earth System Science and Remote Sensing Technologies (CESSRST) City College, City University of New York, Post-doctoral Fellow; New York, NY 10031, USA

² Bio-Optical Oceanography Laboratory, Department of Marine Sciences, University of Puerto Rico-Mayagüez, NOAA-EPP/CESSRST Fellow, Mayagüez, PR 00683, USA; suhey.ortiz@upr.edu (S.O.-R.); roy.armstrong@upr.edu (R.A.A.)

³ Coral Reef Watch NOAA/NESDIS/STAR, College Park, MD 20740, USA; erick.geiger@noaa.gov (E.F.G.); Mark.Eakin@noaa.gov (C.M.E.)

⁴ Earth System Science Interdisciplinary Center/Cooperative Institute for Climate and Satellites-Maryland, University of Maryland, College Park, MD 20740, USA

⁵ NOAA/NOS/NCCOS, Silver Spring, MD 20910, USA; robert.a.warner@noaa.gov

* Correspondence: william.hernandez@upr.edu

Received: 17 January 2020; Accepted: 12 March 2020; Published: 17 March 2020



Abstract: Coastal, benthic communities, such as coral reefs, are at particular risk due to poor water quality caused by hurricanes. In addition to the physical impacts from wave action and storm surge, hurricanes bring significant rainfall resulting in increased runoff from land. Hurricanes Irma and Maria caused record or near-record floods at many locations across Puerto Rico and resulted in major impacts on coastal and benthic ecosystems from heavy rainfall and river discharge. In this study, we use imagery from the moderate resolution Visible Infrared Imaging Radiometer Suite (VIIRS) satellite to quantify the impacts of hurricanes Irma and Maria, which struck Puerto Rico during September 2017, on the water quality of the coastal waters of Puerto Rico using the chlorophyll-*a* (Chl-*a*) and the diffuse attenuation coefficient at 490 nm (K_d490) products. The objectives include: (1) quantify the water quality and light attenuation after the hurricanes; (2) compare this event to the climatology of these parameters, and 3) evaluate long-term exposure and exceedances of various coastal areas to low levels of turbidity. The Chl-*a* inner shelf values increased in 2017 during the months of June (8% above baseline), July (17%), August (5%), September (8%), October (19%), and November (28%) when compared to 2012–2016 baseline data. The values for Chl-*a* concentration reached and exceeded 0.45 $\mu\text{g/L}$ by August 2017 and persisted above that value until December 2017. The K_d490 inner shelf values for 2017 increased (in percent) for the months of June (4% above baseline), July (9%), August (10%), September (5%), October (12%), and November (7%) when compared to 2012–2016 baseline data. The values of K_d490 in August, September, and December 2017 were the highest seen during 2012–2017. Even with the limitations of spatial resolution and loss of data to cloud cover, the 6-year imagery time-series analysis can provide a useful evaluation of the effects of these two hurricanes on the coastal water quality in Puerto Rico, and quantify the exposure of benthic habitats to higher nutrient and turbidity levels.

Keywords: ocean color; hurricanes; remote sensing; water quality; Puerto Rico

1. Introduction

Hurricanes can produce sudden and massive disturbances in estuaries, coastal aquatic, and terrestrial ecosystems around the world [1,2]. The most noticeable impacts to benthic organisms are physical damage. Seagrass can be scoured and uprooted by strong currents, causing them to be transported offshore [3]. For corals, hurricanes can cause breakage, particularly for branching corals, abrasion of the living surface of the corals through the movement of coarse sand and rolling of rubble, and burial of corals through sediment redistribution.

In addition to the physical impacts from wave action, hurricanes bring significant rainfall that leads to increased runoff from land. As development has increased in Puerto Rico, reduced vegetation increases the likelihood of sediments, nutrients, and hazardous substances that can be eroded into coastal waters [4], especially after extreme rain events like hurricanes. Excess sediment, nutrients, and other pollutants can negatively affect seagrass and reef environments principally by decreasing light availability and thereby reducing the photosynthetic capacity for growth [4,5]. Benthic organisms, especially sessile animals, are at particular risk due to poor water quality caused by hurricanes [6]. Coral cover showed a strong correlation with light attenuation, suggesting that deterioration in water quality due to anthropogenic activity could result in reef degradation [7].

Two powerful hurricanes, Irma and Maria, struck Puerto Rico in 2017. At its closest point, Hurricane Irma tracked about 92.6 km (50 nautical miles) to the north of the northern shore of Puerto Rico, delivering rainfall totals between 25.4 cm and 38.1 cm over high elevations in the central portion of the island between September 5–7, 2017 [8] (Figure 1). Hurricane Maria struck Puerto Rico on September 20, 2017 as a Category 4 hurricane (250 kmh (155 mph)) and crossed the island from the southeast to the northwest [9] (Figure 1). Heavy rainfall included one location with nearly 96.5 cm (38 in) of rain. River discharges caused record or near-record floods at many locations across all regions of the island. In addition, major power, transportation, and communication infrastructure were lost.

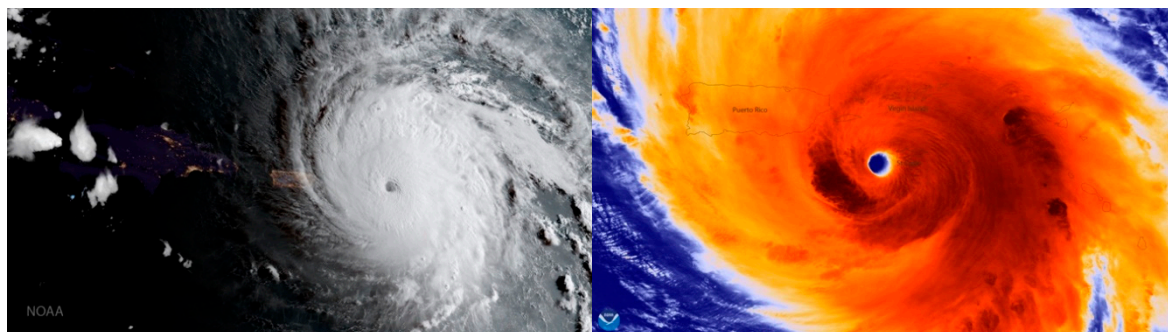


Figure 1. Visible Infrared Imaging Radiometer Suite (VIIRS) satellite images of hurricanes Irma (left) and Maria (right) using I-band 5 (11 μ m). Images courtesy of NOAA National Environmental Satellite, Data, and Information Service (NESDIS).

Satellite ocean color data can provide critical information on coastal water quality conditions after these episodic events. Remote sensing is a cost-effective tool for monitoring large-scale effects [10–13] of hurricanes in the water quality conditions before and after the events. In the case of hurricanes Irma and Maria in Puerto Rico, satellite ocean color data provided the only source of information on water quality and light availability due to lost or damaged in situ sensors and lack of field observations after the storm. These satellite-derived water quality products include the chlorophyll-*a* concentration (Chl-*a*) [14–16] and the water diffuse attenuation coefficient at the wavelength 490 nm (K_d490) [17–19]. The Chl-*a* concentration provides a measurement of phytoplankton biomass, which is related to nutrient status (i.e., productivity), and can be used as an index of water quality. Chl-*a* can also be described as organic material in the water column contributing to light attenuation. K_d490 is an important parameter for water quality since it provides a measure of turbidity (related to the total organic and inorganic matter held in solution and suspension) in the water column and can be used to quantify

light availability and sediment loading for benthic organisms (i.e., coral reefs and seagrasses) [20]. The Chl-*a* algorithm used is based on the ocean color index (OCI) [14] which provides data retrievals for both coastal and oceanic waters. The K_d490 algorithm used (Wang et al., 2009) is particularly useful for turbid coastal and inland waters, when compared with in situ measurements.

In this study, we use moderate-resolution Visible Infrared Imaging Radiometer Suite (VIIRS) satellite images to quantify the impacts of hurricanes Irma and Maria on the quality of coastal waters of Puerto Rico from K_d490 and chlorophyll-*a* products. The objectives include: (1) quantify the water quality and light attenuation after the hurricanes; (2) compare this event to the climatology of these parameters, and (3) evaluate long-term exposure and exceedances of various coastal areas to low levels of turbidity.

2. Data and Methods

2.1. Satellite Data Analysis

This study was focused on the waters surrounding Puerto Rico and used the satellite-derived ocean color products Chl-*a* concentration and K_d490 from VIIRS. This sensor provides daily images at a spatial resolution of 750 m (Figure 2). The study area was divided into four cardinal coastal geographical regions (e.g., North, South, East, and West) to quantify the effects of the hurricanes on water quality in these regions (Figure 3). This segmentation of the study area allowed a refined characterization of the major watersheds, precipitation rates, and important coastal habitats located in those regions. Time-series analysis provided a baseline of these water quality parameters for the regions from 2012–2016 and 2017, to compare directly with the effects of hurricanes.

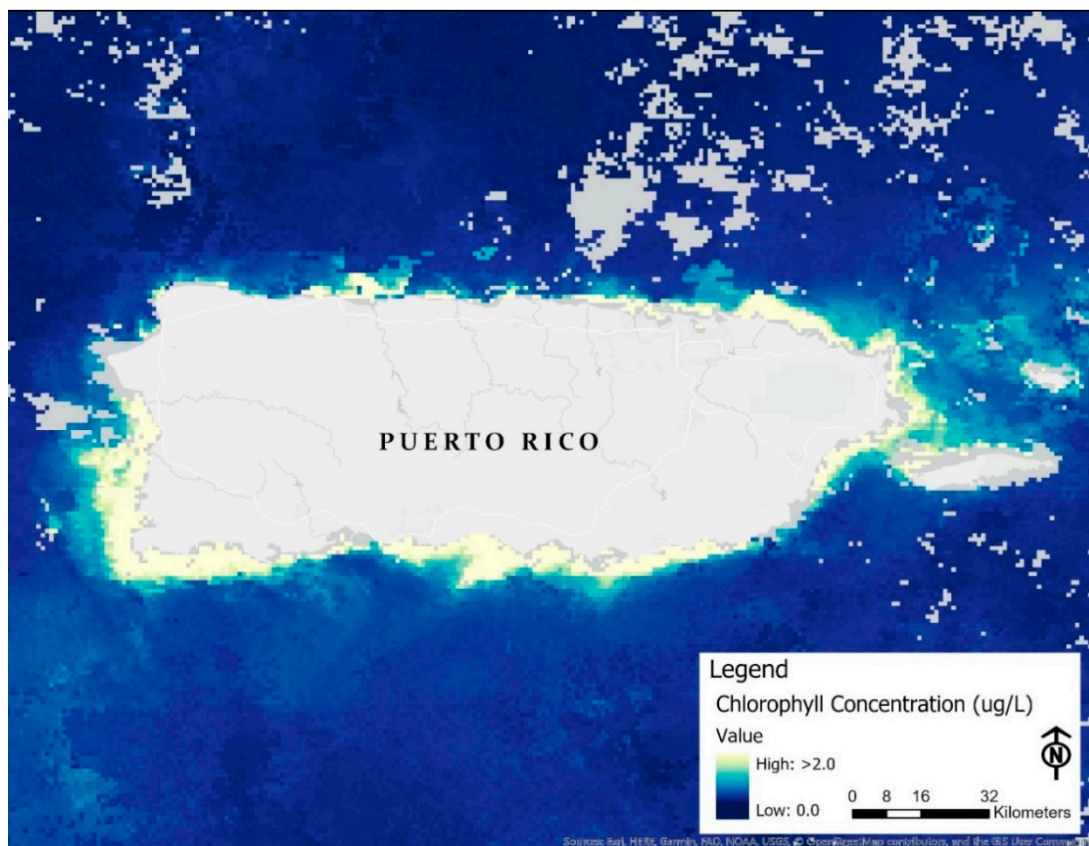


Figure 2. VIIRS satellite map of monthly mean chlorophyll-*a* (Chl-*a*) concentration during September 2017.

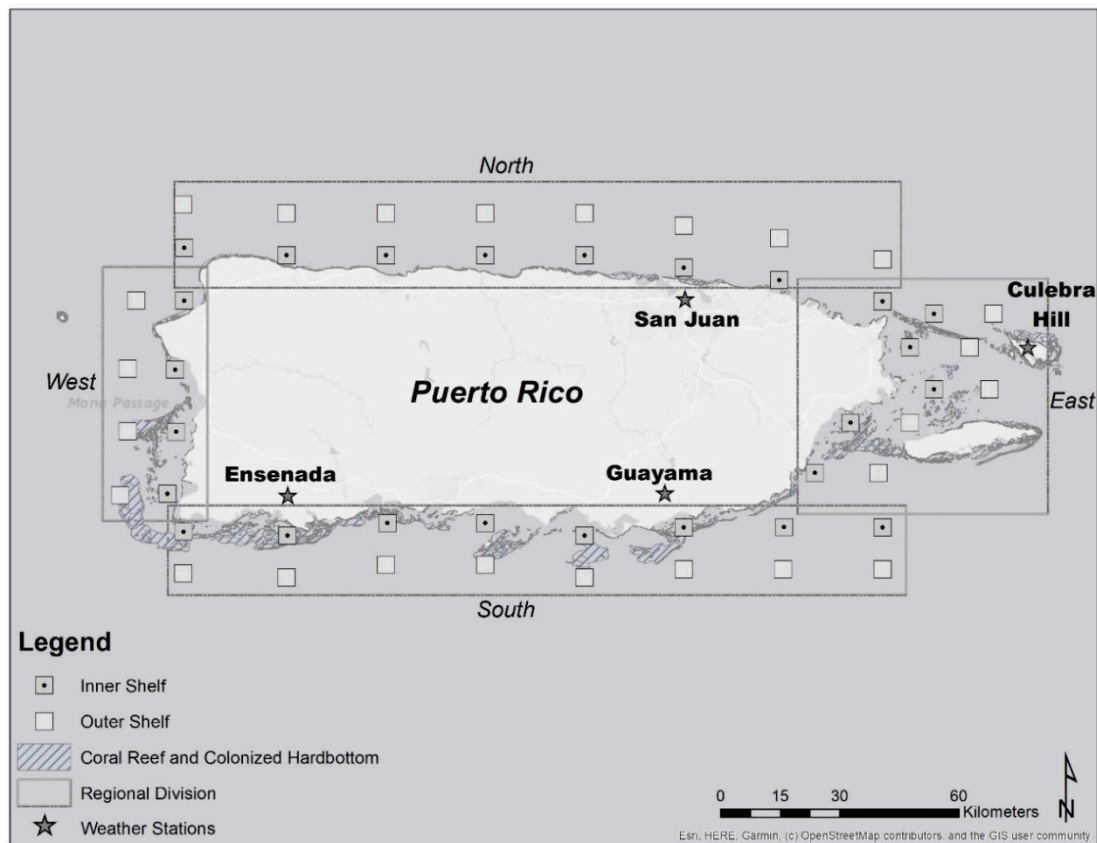


Figure 3. Map of Puerto Rico showing the inner and outer shelf locations, coral reef, and colonized hardbottom [21], regional area divisions, and weather station locations.

Point (pixel) locations were established to characterize the inner shelf and outer shelf contribution to the regional and overall values of $\text{Chl-}a$ and K_d490 , and to quantify these values over coral reef and hard-bottom areas. These points were expanded using a 5×5 pixel box to maximize coverage of the areas within the regions and obtain values from the inner and outer shelf (Figure 3).

The VIIRS images were obtained through the NOAA Coast Watch website (<https://coastwatch.noaa.gov/>) at Level 2 Science Quality accessed in March 2018. These images include a land-mask and a cloud-mask and were gridded and cropped to include only the Puerto Rico regions and further co-registered to ensure pixel overlaps for the time-series. A total of 1825 daily images from January 2012 to December 2017 were analyzed and the images were organized into 72 monthly composites. $\text{Chl-}a$ concentration and K_d490 values were extracted from the images using a gridded point selection within the regions (Figure 3). The images were processed and stored in NetCDF (.nc) format and exported in GeoTiff (.tif) format for use in other GIS mapping platforms.

The 2012–2016 monthly means for the $\text{Chl-}a$ concentrations and K_d490 were used as the baseline values for these parameters and then compared with the monthly averages from 2017 to evaluate potential anomalous water quality areas around Puerto Rico.

In addition to the changes to water quality produced by extreme events, the values were analyzed based on the coastal water quality standards that have been adopted by both national and international jurisdictions. No coastal water quality standards have been adopted by Puerto Rico for the chlorophyll concentration or light attenuation so the State of Hawai'i [22] and the Great Barrier Reef Marine Park (GBRMP) [23] standards were used for reference. The threshold values of chlorophyll concentration for open coastal waters were established at 0.15 to 0.30 $\mu\text{g/L}$ for Hawai'i coastal waters and 0.45 $\mu\text{g/L}$ for the GBRMP. For the K_d490 values, only State of Hawai'i provides values for light attenuation (K_d) at 0.1 m^{-1} for open coastal waters. The values of $\text{Chl-}a$ 0.45 $\mu\text{g/L}$ and K_d490 0.1 m^{-1} were used as

threshold values for this study and values above these thresholds are recognized globally as adverse for coral reefs [23].

2.2. Precipitation Analysis

Precipitation data were obtained from the NOAA National Center for Environmental Information (NCEI) Global Summary of the Month product that provided a global summary of the precipitation and temperature data. Four stations were chosen to represent the regions selected. For the North (San Juan, Station ID: RQW00011641), for the East (Culebra Hill, Station ID: RQC00666343), for the South (Guayama, Station ID: RQC00664193), and for the West (Ensenada, Station ID: RQC00665693). The selection was based on the locations of the hurricane-impacted habitats including corals, seagrass beds, mangroves, and other benthic ecosystems, and data availability for the stations from 2012–2017 (Figure 3). Some precipitation values for 2013 were absent for Culebra. For any absent data, the monthly average for 2012 to 2016 was calculated excluding the missing data points. Precipitation data were then correlated to Chl-*a* and K_d490 concentration values across Puerto Rico.

3. Results

3.1. Precipitation Values

During September and October 2017 there was significantly higher precipitation than the monthly average in all four regions over 2012–2016 (Figure 4). This higher rainfall was mainly due to the impact of hurricanes Irma and Maria during September 5, 2017 and September 20, 2017, respectively. Increased rainfall throughout the month of October also contributed to the peaks observed, particularly for the South region.

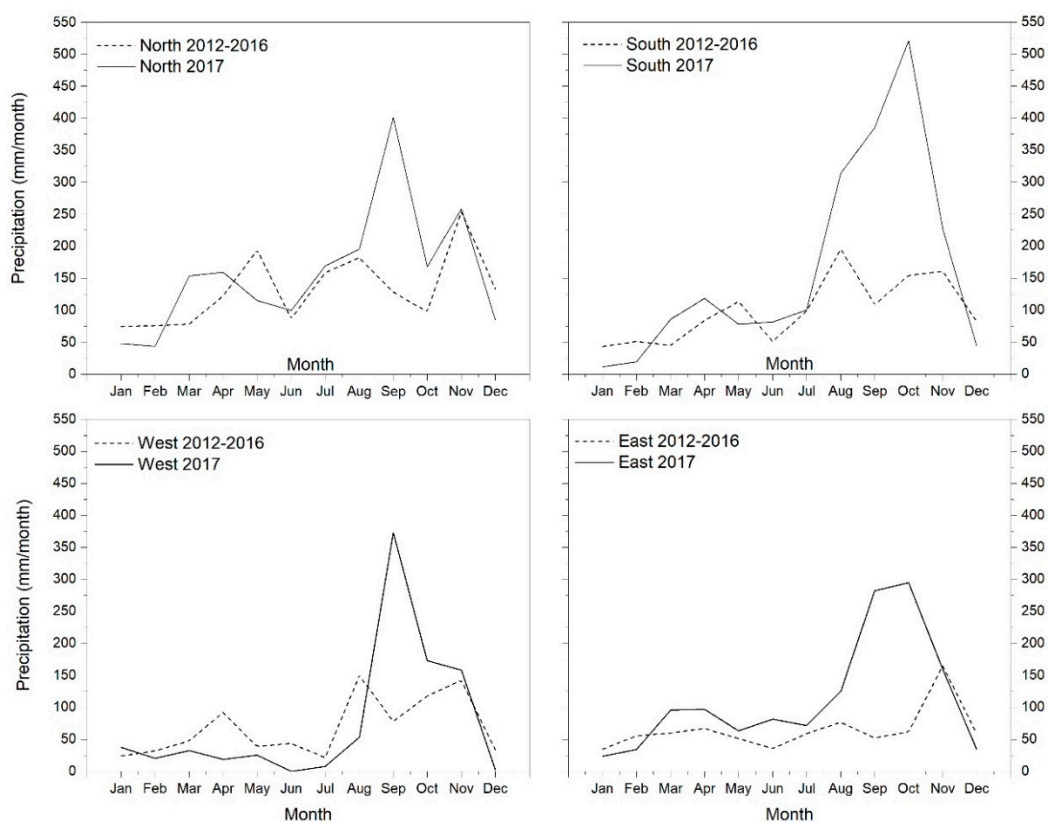


Figure 4. Monthly averaged precipitation for the North, South, West, and East during 2012–16 baseline period and for 2017.

The South region showed the highest amount of precipitation, followed by North, East, and West. The North and West regions experienced a significant increase in precipitation starting in August that began to decrease in October 2017. The East and South regions also experienced a major increase in rainfall in August but did not decrease until November. The West region showed lower precipitation values from February 2017 to early August 2017 compared to 2012–2016 (Figure 4).

3.2. Regional and Monthly Pre- and Post-Hurricane Water Quality

3.2.1. Chl-*a* Concentrations

An increase in Chl-*a* concentration was observed from August–November 2017 for all regions (Figure 5). Chl-*a* concentration spikes may not have been observed in the East and North because baseline values were relatively high. When all regions are considered, an increase in Chl-*a* concentration for 2017 positively correlates with an increase in precipitation ($r_s = 0.52$; $p = 0.080$). The East region showed the highest contribution to the overall chlorophyll-*a* value for the island, followed by the North, West, and South regions (Figure 5) for both 2012–16 and 2017. The West region showed lower precipitation values from February 2017 to the beginning of August 2017 as compared to 2012–2016; during this time, Chl-*a* concentrations were lower than the average for 2012–2016 as well. The East region had higher rainfall values in 2017 overall as compared to 2012–2016; this may have contributed to increased Chl-*a* concentration for 2017. Precipitation influences the Chl-*a* concentration for the north region (2017 $r_s = 0.73$; $p = 0.006$, 2012–16 $r_s = 0.60$; $p = 0.038$) and the south region (2017 $r_s = 0.40$; $p = 0.191$, 2012–16 $r_s = 0.60$; $p = 0.036$).

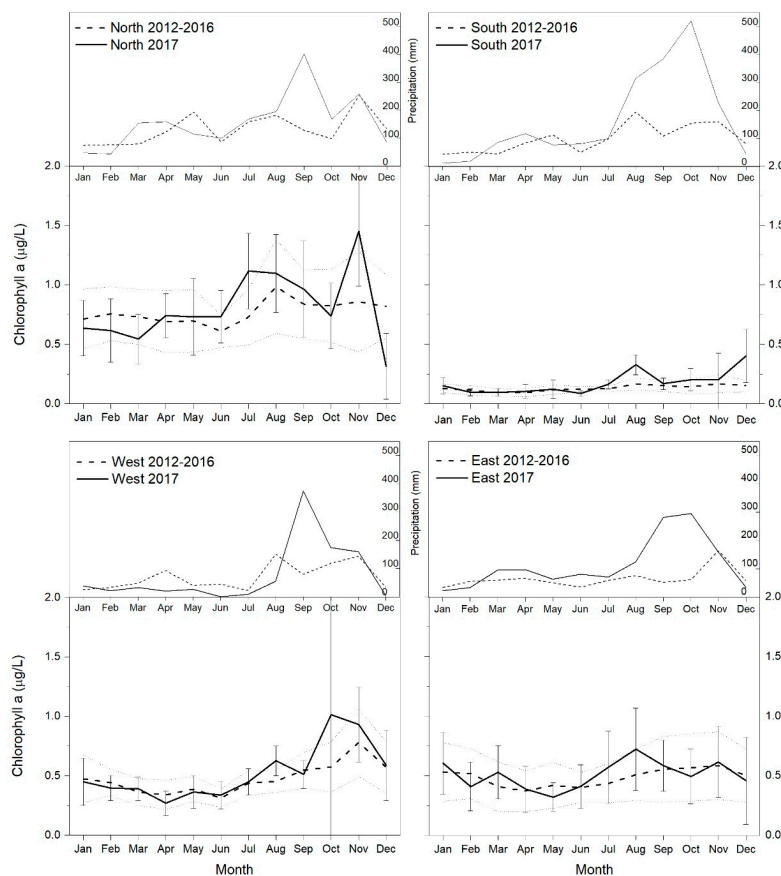


Figure 5. Monthly averaged precipitation and Chl-*a* concentration with standard deviation by regions for 2012–16 baseline period and 2017.

Chl-*a* concentrations were analyzed monthly for each year to identify the differences between years and the seasonal trends (Figure 6). The higher Chl-*a* values were observed from July to December 2017 when considering the average of all regions. Chl-*a* concentration exceeded 0.45 µg/L by August 2017 and persisted until December 2017. Chl-*a* concentration values above 0.45 µg/L were also present in previous years but never exceeded this threshold for more than 5 months. Average Chl-*a* concentration for Puerto Rico showed an increase in 2017 when compared with previous values from 2012–2016 especially in the peak of the rainy season (August–November) (Figure 6). The months that showed an increase over the previous baseline values are July (17% higher than baseline), August (36%), September (20%), October (9%), November (14%), and December (13%).

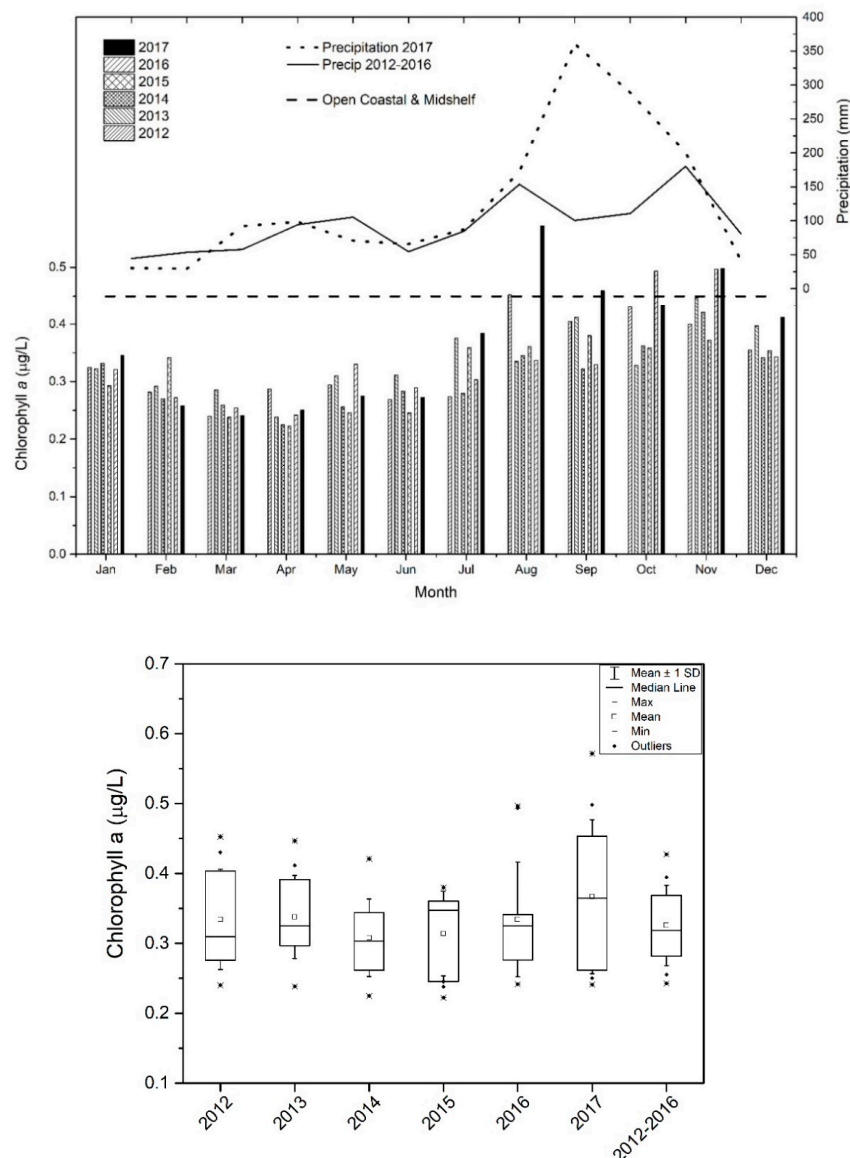


Figure 6. Monthly comparison of the Chl-*a* concentration for all regions (µg/L) showing the yearly distribution from 2012–2017 with associated precipitation data (top). The year 2017 is filled in black. The dashed line for 0.45 µg/L represents the chlorophyll threshold for open coastal and mid-shelf waters [23]. (Bottom) Box plot showing yearly statistics of the Chl-*a* concentration for all regions.

3.2.2. K_d490

The K_d490 values were analyzed by month per year to compare the differences between years and seasonal trends. The East region showed the highest contribution to the overall K_d490 value for the

island, followed by the North, West, and South regions (Figure 7). Precipitation contributes to a greater degree to the K_d490 values in the South (2012–16, $r_s = 0.79$; $p = 0.001$) and North (2017 $r_s = 0.68$; $p = 0.014$) regions. The East region had higher rainfall values in 2017 overall as compared to 2012–2016; this correlated with increased K_d490 values for 2017 ($r_s = 0.44$; $p = 0.459$). Overall, an increase in K_d490 correlated with an increase in precipitation (2017, $r_s = 0.46$; $p = 0.124$), 2012–16, $r_s = 0.53$; $p = 0.075$). Additionally, there is a strong correlation between the Chl-*a* and K_d490 ($r_s = 0.99$; $p = 0$) products for the complete time series.

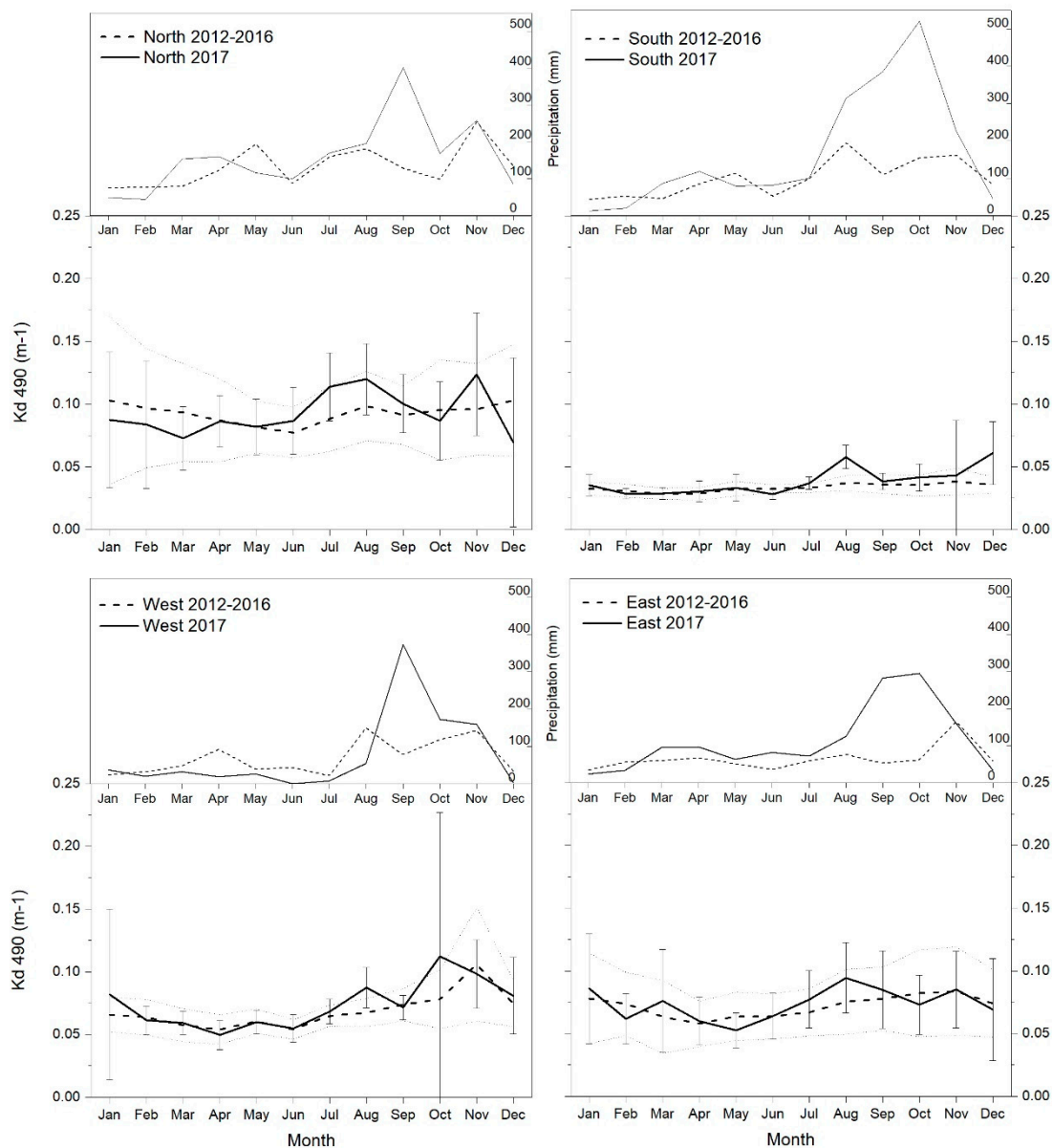


Figure 7. Monthly averaged precipitation and K_d490 with standard deviation by regions for 2012–16 baseline period and 2017.

Higher values were present from July to December 2017 when considering all regions (Figure 7). The values for K_d490 reached and exceeded 0.06 m^{-1} by July 2017 and persisted by December 2017. K_d490 values above the 0.06 m^{-1} were also present in previous years, but the 2017 values for the months of August, September, and December are the highest for all the time series from 2012–2017. The values of K_d490 for Puerto Rico show an increase for 2017 when compared with values from 2012–2016, especially in the peak of the rainy season (August–November) (Figure 8). The months

that show an increase from the previous baseline values are July (10% higher than baseline), August (28%), September (15%), October (5%), November (7%), and December (12%). The values for K_d490 concentration from August to December 2017 were all above 0.06 m^{-1} .

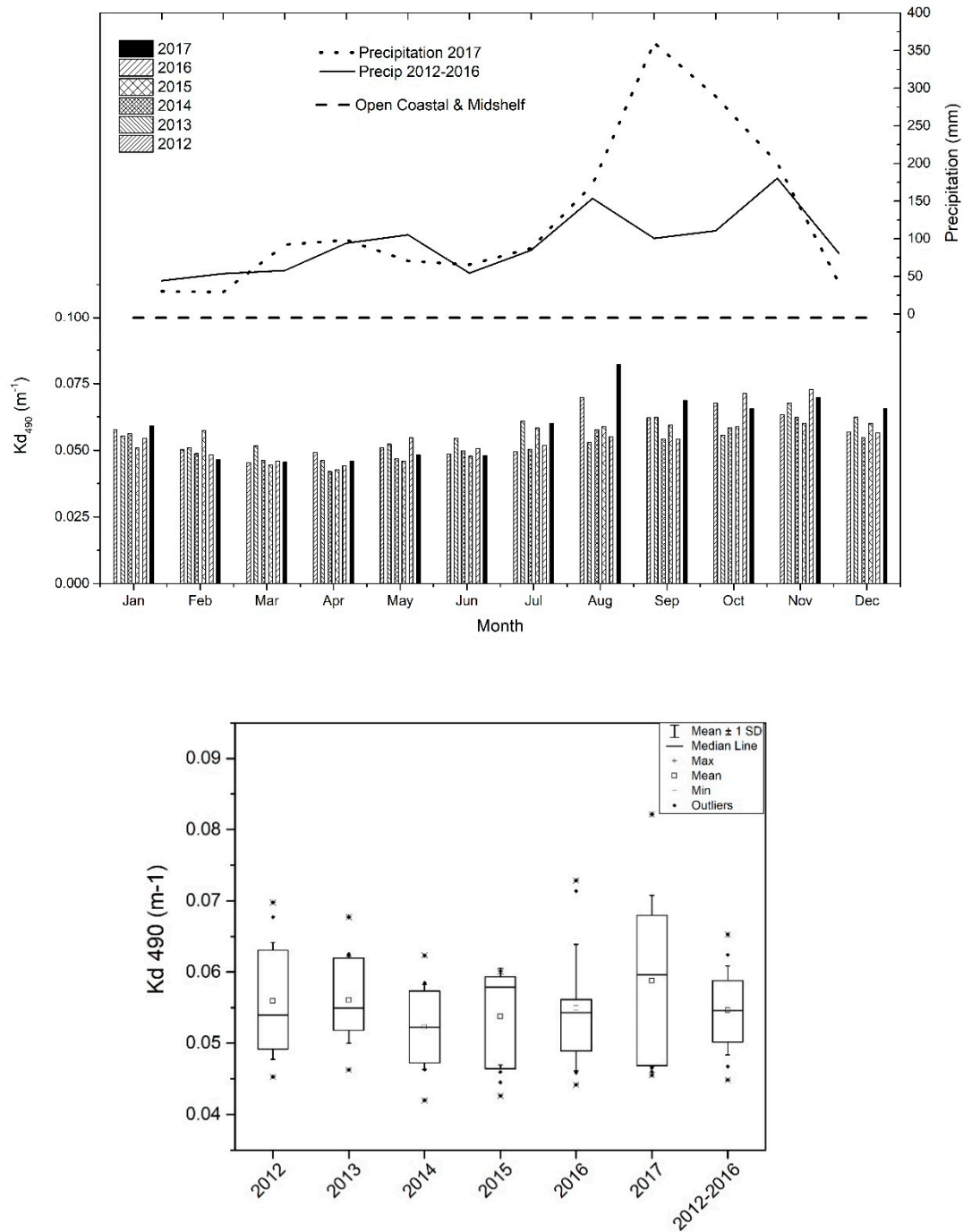


Figure 8. Monthly comparison of K_d490 values showing the yearly distribution from 2012–2017 with associated precipitation data (top). The year 2017 is filled in black. The dashed line for 0.1 m^{-1} represents the K_d490 value threshold for open coastal waters [22]. (Bottom) Box plot showing yearly statistics of K_d490 for all regions.

3.3. Inner Shelf vs Outer Shelf Pixels

Pixel point locations were evaluated to quantify the difference from coastal to oceanic waters around Puerto Rico. The pixel locations are broken out into inner shelf and outer shelf regions (Figures 9 and 10). Approximately 74% of the average value of Chl-*a* for Puerto Rico (0.55 µg/L) was driven by the inner shelf pixel locations, where 26% was attributed to the outer shelf locations. A small variation ($\pm 3\%$) was found in the contribution of the inner vs. outer shelf to the average value of Chl-*a* for all Puerto Rico, even when considering regional and yearly distributions. These pixel locations were also analyzed by month and compared between 2012–2016 and 2017 data (Figure 9). Chl-*a* values for outer shelf locations remained below 0.45 µg/L except for the months of July and August of 2017. The values for the inner shelf pixels remained below the 0.8 µg/L value from January to June for both 2017 and 2012–2016 data. The inner shelf values for 2017 displayed an increase (in percent) for the months of June (8% from baseline), July (17%), August (5%), September (8%), October (19%), and November (28%) when compared to 2012–2016 data.

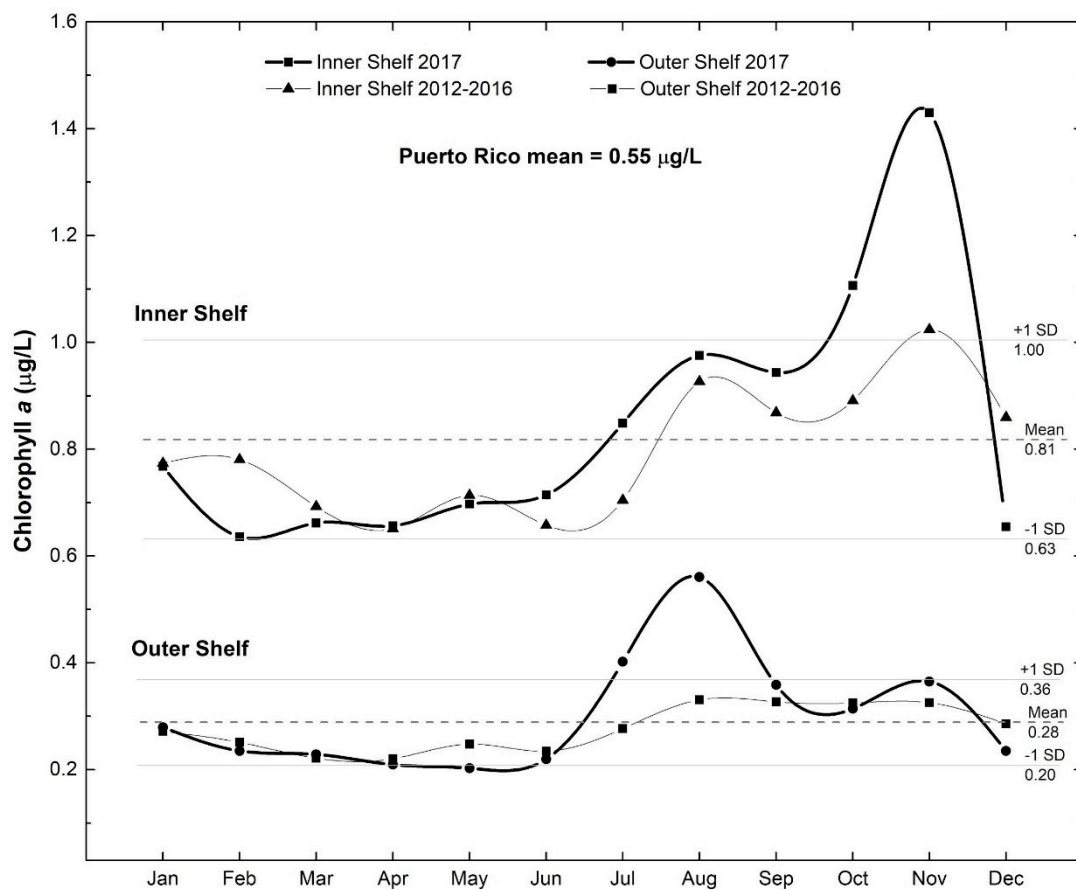


Figure 9. Chlorophyll-*a* concentration for inner shelf and outer shelf of Puerto Rico waters.

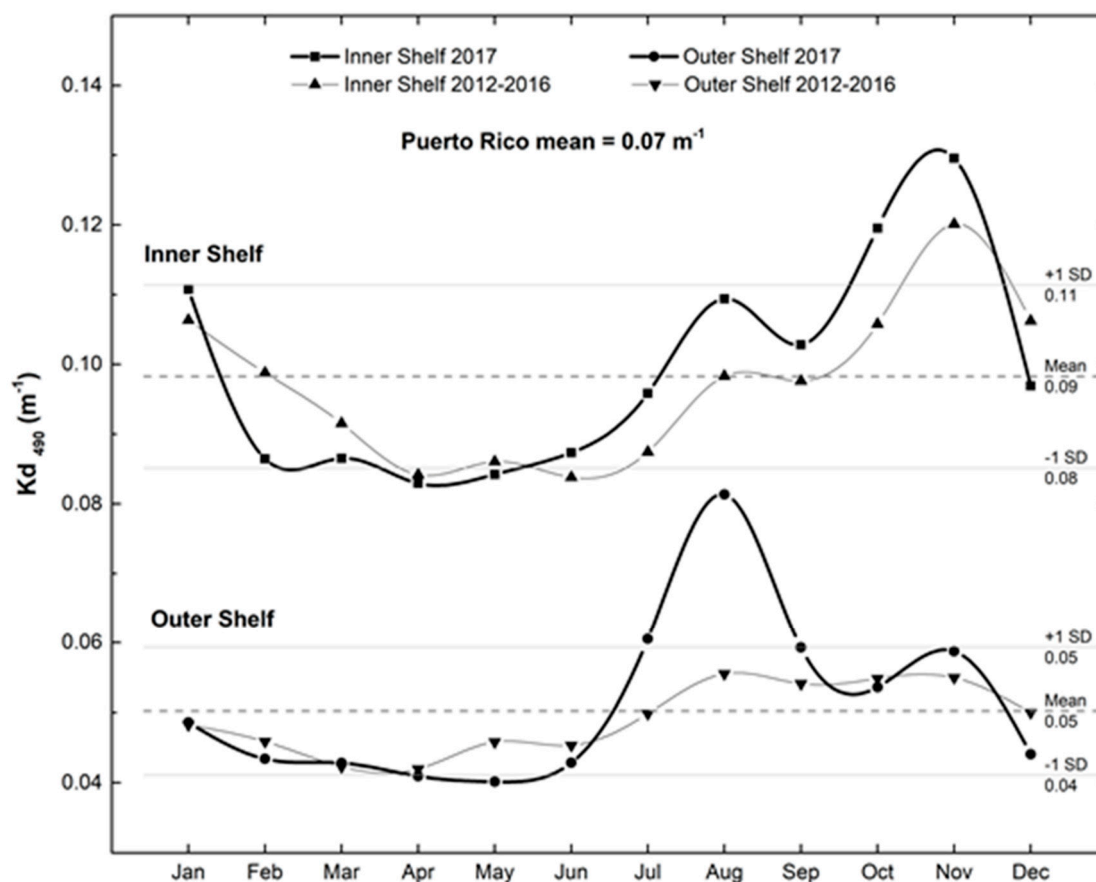


Figure 10. K_d490 for inner shelf and outer shelf of Puerto Rico waters.

For the K_d490 values, approximately 70% of the average value for Puerto Rico (0.07 m^{-1}) were driven by the inner shelf pixel locations, while the remaining 30% was from outer shelf pixel locations. There was little variation ($\pm 3\%$) in the contribution of the inner vs. outer shelf to the average value of K_d490 for all Puerto Rico, even when considering regional and yearly distributions. These pixel locations were also analyzed by month and compared from 2012–2016 to 2017 data (Figure 10). The values for outer shelf locations remained below 0.06 m^{-1} except for the months of July and August of 2017. The inner shelf values remained below the 0.10 m^{-1} value from February to July for both 2017 and 2012–2016 data. The inner shelf values for 2017 increased (in percent) during the months of June (4% from baseline), July (9%), August (10%), September (5%), October (12%), and November (7%) when compared to 2012–2016 data.

4. Discussion

Hurricanes Irma and Maria Effects on Water Quality

Hurricane Maria's 24-hr rainfall intensity was undoubtedly the highest for any tropical cyclone in Puerto Rico since 1898 [24]. This event represented a 13% increase in the island-wide 24-hour rainfall rates, which is within the range of predicted increases associated to climate change both locally and worldwide [24]. The precipitation data for our selected stations also shows an increase in 2017, especially during the months of August to October. Such extreme precipitation events from tropical cyclones can alter the coastal water quality regimes [25]. Higher mean, median, and maximum values were observed for both Chl-*a* and K_d490 when compared to previous years (Figures 6 and 8).

The highest values of both Chl-*a* and K_d490 were present in August 2017, just before the hurricane impact, which corresponds with an increase in precipitation during that same month when compared

with 2012–2016 values. Regional values also show a dramatic increase by the month of August 2017 when compared to 2012–2016. According to National Weather Service (NWS) San Juan weather report for 2017, July and August showed an increase in monthly precipitation of 53.3 mm and 61.5 mm respectively from the normal (1981–2010) [26] which explain the higher values for both Chl-*a* and K_d490 .

In addition to increased light attenuation, sediment reaching the coast from runoff can smother corals and has been shown to have a detrimental effect on coral recruitment, decrease calcification, decrease net productivity of corals, and reduce rates of reef accretion [27]. In addition, introducing nutrients and high turbidity to what is generally an oligotrophic system, combined with decreased grazing due to overfishing, can promote the growth of macroalgae which may then outcompete corals for space on reefs [28]. To put these values into context, impairment thresholds for Chl-*a* and water clarity from the GBRMP and State of Hawai'i water quality standards were shown in previous figures (Figures 5 and 7–9). Thresholds of 0.45 $\mu\text{g/L}$ were used for Chl-*a*, and 0.1 m^{-1} for K_d490 coefficients for open coastal waters. For both indicators, inner shelf points showed values above these thresholds before and after the hurricanes and these values exceeded thresholds globally recognized as adverse for coral reefs [23]. One alarming factor is that the mean Chl-*a* value for Puerto Rico for the complete time-series (2012–2017) was 0.55 $\mu\text{g/L}$, higher than the established threshold even when considering inner/outer shelf pixels, suggesting chronically impaired water quality. These data can provide key information for management to establish water quality thresholds for coastal waters, as well as prioritize restoration efforts of watershed and coral reef areas.

When comparing the inner and outer shelf pixel values of Chl-*a* and K_d490 , this follows the distinct neritic to oceanic gradients of water turbidity observed for the oceanic waters surrounding Puerto Rico [5]. This suggests that areas closer to shore experienced higher levels of degraded water. 9 of the 25 inner shelf pixels were over coral reef and colonized hardbottom areas (Figure 3), where higher values of both Chl-*a*, and K_d490 were present and persisted for various months. Miller [10] used total suspended matter (TSM) from the Sentinel 3 Ocean Color Land Instrument (OLCI) to find that island-wide mean TSM increased 2.2 times (5.57 mg/L to 12.39 mg/L) between before and two weeks after Hurricane Maria's strike, rapidly dropping by November (5–6 mg/L), and reaching normal levels by February 2018 (2.14 mg/L). Degraded water quality conditions persisted for months after the hurricanes as shown by our Chl-*a* and K_d490 values. No TSM products are available from VIIRS to compare these results. Additionally, the North and East regions contributed to the high values of both Chl-*a* and K_d490 since those regions contain Puerto Rico's major rivers, while the smallest rivers are mainly found along the south coast [29].

Our results for Chl-*a* and K_d490 did not find strong overall positive correlations with precipitation values. This may be due to a non-linear relationship between precipitation and surface runoff as a result of reduced foliage interception due to hurricane defoliation, which did not exceed 1.0 kg/m^2 in the month preceding Maria, but reached 3 times this value before comparatively drier conditions arrived in December [10]. Warne [29] estimated that 57 % of the mean annual precipitation (911 mm/yr) in Puerto Rico is discharged to the coast as runoff due to steep gradients, relatively shorter river lengths, and low water holding capacity. These surface hydrology characteristics and the fact that both the precipitation and satellite data were summarized into monthly values, reduce the potential lag between precipitation and satellite ocean color measurements. In addition, there were few stations with reliable historical records of precipitation data per region that could be correlated with the 2012–2017 time series. This may have contributed to the low correlation values for some regions, due to an incomplete representation of the total precipitation values for the regions.

In addition, the peak values for both Chl-*a* and K_d490 for September–October 2017 may have been underestimates due to limited numbers of retrievals resulting from high cloud cover. According to Mikelsons and Wang [30], the most significant limiting factors in satellite ocean color data retrievals is cloud cover, and large cyclone systems can prevent ocean color data retrievals over vast areas for several days. In fact, a prolonged period of cloudy conditions followed these storms. This reduction

in cloud-free imagery is magnified by the afternoon timing of overpass of satellites flying the VIIRS instrument. During that season, cloud formation is generally high due to local trade winds and orographic effects. “Blended” Chl-*a* and K_d490 products from a combination of moderate resolution sensors (i.e., SeaWiFS, MODIS, JPSS, OLCI) at full resolution (≤ 1 km), with different satellite observation times may improve the amount of cloud-free observations in near-shore environments, as would the presence of ocean color instruments on geostationary satellites.

5. Conclusions

Moderate-resolution satellite imagery, such as VIIRS can provide a reliable method to evaluate potential habitat exposure to degraded water quality without conducting extensive in-situ water quality monitoring. Even with the limitations of spatial resolution and loss of data due to cloud cover, moderate-resolution imagery time-series analysis has provided a useful evaluation of the effects of the hurricanes on the coastal water quality in Puerto Rico, and the potential exposure of benthic habitats to higher turbidity waters. The regions around Puerto Rico experienced extreme and prolonged levels of pollution exceeding established thresholds for coastal and open ocean areas that contain coral and seagrass habitats. This pollution came from multiple sources including sediment from the extensive landslides and untreated sewage from the persistent losses of power across the island and use of combined sewer systems that collect rainwater runoff, domestic sewage, and industrial wastewater into a single system. Depending on the magnitude and duration of the pollution, and the condition of the habitat prior to the hurricane, these exposures likely led to a range of habitat-scale impacts including, but not limited to inhibition of light penetration needed to support photosynthesis, physical smothering of the habitat by sediment, and excessive algal growth, which will outcompete coral reefs and seagrass. Those habitats that were previously impaired due to chronic pollution are particularly susceptible to this threat.

Water quality exceedances and corresponding habitat exposures varied across the inner shelf and outer shelf locations (i.e., coastal, oceanic) and regions (i.e., North, South, East, West). For inner shelf locations, many of the observed baseline and post-hurricane values for Chl-*a* and K_d490 are above thresholds for impairment recognized by coral jurisdictions around the globe. Outer shelf locations generally show lower values. Degraded coastal water quality has the highest potential of impact and these were present close to shore, where coral reef and other critical habitats are located. In addition, some regions suffered more severe hurricane impact than others. In the east region, for instance, turbidity was higher than in other regions prior to the hurricanes, therefore post-hurricane differences in degraded water quality were masked in our change analysis. The results from this project can be used as a guideline to establish local thresholds for water quality of these parameters in the coastal areas of Puerto Rico taking into consideration suggested long-term increases in precipitation from altered extreme weather scenarios.

Author Contributions: W.J.H. conceived and designed the study, W.J.H. and S.O.-R. performed the experiments, conducted and performed data processing and analysis; R.A.A., C.M.E., E.F.G., and R.A.W. contributed to data collection; W.J.H. wrote the manuscript, with all authors contributing to manuscript revisions; W.J.H. and R.A.A. attracted funds for the project. All authors have read and approved the manuscript.

Funding: This study was supported in part by The National Oceanic and Atmospheric Administration –Cooperative Science Center for Earth System Sciences and Remote Sensing Technologies (NOAA-CESSRST) under the Cooperative Agreement Grant # NA16SEC4810008. The authors would like to thank The City College of New York, NOAA-CESSRST program and NOAA Office of Education, Educational Partnership Program for full fellowship support. The statements contained within the manuscript/research article are not the opinions of the funding agency or the U.S. government but reflect the author’s opinions. NOAA Coral Reef Watch staff were fully supported, and this study was partially supported, by NOAA grant NA19NES4320002 (Cooperative Institute for Satellite Earth System Studies) at the University of Maryland/ESSIC. The scientific results and conclusions, as well as any views or opinions expressed herein, are those of the author(s) and do not necessarily reflect the views of NOAA or the Department of Commerce.

Acknowledgments: The authors would like to thank Lisa Vandiver, Anne Kitchell and Roberto Viqueira for their contributions and support to this project.

Conflicts of Interest: The authors declare no conflict of interest. The funders had no role in the design of the study; in the collection, analyses, or interpretation of data; in the writing of the manuscript, or in the decision to publish the results.

References

1. Greening, H.; Doering, P.; Corbett, C. Hurricane impacts on coastal ecosystems. Estuaries and coasts, part A: Hurricane impacts on coastal ecosystems. *J. Coast. Estuar. Res. Fed.* **2006**, *29*, 877–879. [[CrossRef](#)]
2. Valiela, I.P.; Peckol, C.; D'Avanzo, J.; Kremer, D.; Hersh, K.; Foreman, K.; Lajtha, B.; Seely, W.R.; Geyer, I.; Crawford, R. Ecological effects of major storms on coastal watersheds and coastal waters: Hurricane Bob on Cape Cod. *J. Coast. Res.* **1998**, *14*, 218–238.
3. Hernandez-Cruz, L.R.; Purkis, S.J.; Riegl, B. Documenting decadal spatial changes in seagrass and *Acropora palmatta* cover by aerial photography analysis in Vieques, Puerto Rico: 1937–2000. *Bull. Mar. Sci.* **2006**, *2*, 401–414.
4. Hernández-Delgado, E.A. The emerging threats of climate change on tropical coastal ecosystem services, public health, local economies and livelihood sustainability of small islands: Cumulative impacts and synergies. *Mar. Pollut. Bull.* **2015**, *101*, 5–28. [[CrossRef](#)]
5. García-Sais, J.R.; Williams, S.M.; Amirrezvani, A. Mortality, recovery, and community shifts of scleractinian corals in Puerto Rico one decade after the 2005 regional bleaching event. *PeerJ* **2017**, *5*, e3611. [[CrossRef](#)]
6. Mallin, M.A.; Corbett, C.A. How Hurricane attributes determine the extent of environmental effects: Multiple hurricanes and different coastal systems. *Estuaries Coasts* **2006**, *29*, 1046–1061. [[CrossRef](#)]
7. Bejarano, I.; Apeldoorn, R. Seawater turbidity and fish communities on coral reefs of Puerto Rico. *Mar. Ecol. Prog. Ser.* **2013**, *474*, 217–226. [[CrossRef](#)]
8. Cangialosi, J.P.; Latto, A.S.; Berg, R. National Hurricane Center Tropical Cyclone Report Hurricane Irma (AL112017). 2018. Available online: https://www.nhc.noaa.gov/data/tcr/AL112017_Irma.pdf (accessed on 20 August 2018).
9. Pasch, R.J.; Penny, A.B.; Berg, R. National Hurricane Center Tropical Cyclone Report Hurricane María (AL152017). 2018. Available online: https://www.nhc.noaa.gov/data/tcr/AL152017_María.pdf (accessed on 20 August 2018).
10. Miller, P.W.; Kumar, A.; Mote, T.L.; Moraes, F.D.S.; Mishra, D.R. Persistent hydrological consequences of Hurricane María in Puerto Rico. *Geophys. Res. Lett.* **2019**, *46*, 1413–1422. [[CrossRef](#)]
11. Hu, T.; Smith, R.B. The Impact of Hurricane María on the Vegetation of Dominica and Puerto Rico Using Multispectral Remote Sensing. *Remote Sens.* **2018**, *10*, 827. [[CrossRef](#)]
12. Shi, W.; Wang, M. Observations of a Hurricane Katrina-induced phytoplankton bloom in the Gulf of Mexico. *Geophys. Res. Lett.* **2007**, *34*, 11607. [[CrossRef](#)]
13. Gilbes, F.; Armstrong, R.A.; Webb, R.M.; Müller-Karger, F.E. SeaWifs helps assess hurricane impact on phytoplankton in caribbean sea. *Eos Trans. Am. Geophys. Union* **2001**, *82*, 529. [[CrossRef](#)]
14. Wang, M.; Son, S. VIIRS-derived chlorophyll-a using the ocean color index method. *Remote Sens. Environ.* **2016**, *182*, 141–149. [[CrossRef](#)]
15. Hu, C.; Lee, Z.; Franz, B.A. Chlorophyll-a algorithms for oligotrophic oceans: A novel approach based on three-band reflectance difference. *J. Geophys. Res.* **2012**, *117*. [[CrossRef](#)]
16. O'Reilly, J.E.; Maritorena, S.; Mitchell, B.G.; Siegel, D.A.; Carder, K.L.; Garver, S.A.; Kahru, M.; McClain, C.R. Ocean color chlorophyll algorithms for SeaWiFS. *J. Geophys. Res.* **1998**, *103*, 24937–24953. [[CrossRef](#)]
17. Wang, M.; Son, S.; Harding, L.W., Jr. Retrieval of diffuse attenuation coefficient in the Chesapeake Bay and turbid ocean regions for satellite ocean color applications. *J. Geophys. Res.* **2009**, *114*. [[CrossRef](#)]
18. Morel, A.H.Y.; Gentili, B.; Werdell, P.J.; Hooker, S.B.; Franz, B.A. Examining the consistency of products derived from various ocean color sensors in open ocean (Case 1) waters in the perspective of a multi-sensor approach. *Remote Sens. Environ.* **2007**, *111*, 69–88. [[CrossRef](#)]
19. Lee, Z.P.; Du, K.; Arnone, R. A model for the diffuse attenuation coefficient of downwelling irradiance. *J. Geophys. Res.* **2005**, *110*. [[CrossRef](#)]
20. Kirk, J.T.O. *Light and Photosynthesis in Aquatic Ecosystems*; Cambridge University Press: Cambridge, UK, 2011.

21. Kendall, M.S.C.R.; Krueger, K.R.; Buja, J.D.; Christensen, M.; Finkbeiner, R.A.; Warner Monaco, M.E. NOAA Technical Memorandum NOS NCCOS CCMA 152 (On-line). Methods Used to Map the Benthic Habitats of Puerto Rico and the U.S. Virgin Islands. 2001. Available online: <http://biogeos.nos.noaa.gov/projects/mapping/caribbean/startup.htm> (accessed on 21 November 2019).
22. Water Quality Standards (WQS). Hawaii Administrative Rules (HAR). Amendment and Compilation of Chapter 11–54. State of Hawai‘i Department of Health. Available online: <https://www.epa.gov/wqs-tech/water-quality-standards-regulations-hawaii> (accessed on 22 November 2019).
23. (GBRMPA) Great Barrier Reef Marine Park Authority. *Water Quality Guidelines for the Great Barrier Reef Marine Park*; Great Barrier Reef Marine Park Authority: Townsville, Australia, 2010; p. 99.
24. Ramos-Scharrón, C.E.; Arima, E. *Hurricane María’s Precipitation Signature in Puerto Rico: A Conceivable Presage of Rains to Come*; Scientific Reports; Nature Research: London, UK, 2019.
25. Keellings, D.; Hernández Ayala, J.J. Extreme rainfall associated with Hurricane María over Puerto Rico and its connections to climate variability and change. *Geophys. Res. Lett.* **2019**, *46*, 2964–2973. [[CrossRef](#)]
26. NWS San Juan. Climate Review for Puerto Rico and the U.S. Virgin Islands. Climate Reports from the Weather Forecast Office San Juan. 2017. Available online: https://www.weather.gov/media/sju/climo/monthly_reports/2017/2017.pdf (accessed on 8 February 2020).
27. Rogers, C.S. Responses of coral reefs and reef organisms to sedimentation. *Mar. Ecol.* **1990**, *62*, 185–202. [[CrossRef](#)]
28. Scheffer, M.S.; Carpenter, J.A.; Foley, C.; Folke Walker, B. Catastrophic shifts in ecosystems. *Nature* **2001**, *413*, 591–596. [[CrossRef](#)]
29. Warne, A.G.; Webb, R.M.T.; Larsen, M.C. Water, sediment, and nutrient discharge characteristics of rivers in Puerto Rico, and their potential influence on Coral Reefs. Available online: <http://pubs.usgs.gov/sir/2005/5206/> (accessed on 30 January 2007).
30. Mikelsons, K.; Wang, M. Optimal satellite orbit configuration for global ocean color product coverage. *Opt. Express* **2019**, *27*, A445–A457. [[CrossRef](#)] [[PubMed](#)]



© 2020 by the authors. Licensee MDPI, Basel, Switzerland. This article is an open access article distributed under the terms and conditions of the Creative Commons Attribution (CC BY) license (<http://creativecommons.org/licenses/by/4.0/>).